European Journal of Applied Sciences – Vol. 13, No. 05
Publication Date: October 06, 2025
DOI:10.14738/aivp.1305.19448.

Yang, C.-C., Lu, J.-Q., Tsai, H. Y., & Andres, J. C. (2025). The Numerical Study on the Multi-Stage Cold Forming Process of Hexalobular Socket Torx Nuts. *European Journal of Applied Sciences, Vol - 13(05).* 266-277.

The Numerical Study on the Multi-Stage Cold Forming Process of Hexalobular Socket Torx Nuts

Chih-Cheng Yang
Department of Mechanical and Automation Engineering,
Taiwan Steel University, Taiwan

Jian-Qing Lu
Graduate School of Mechatronic Science and Technology,
Taiwan Steel University, Taiwan

Hsiu Ying Tsai
Graduate School of Mechatronic Science and Technology,
Taiwan Steel University, Taiwan

Jhonel Cortez Andres
Graduate School of Mechatronic Science and Technology,
Taiwan Steel University, Taiwan

ABSTRACT

In this study, a multi-stage cold forming process for the manufacture of hexalobular socket Torx nuts is studied numerically with AISI 1022 carbon steel. The cold forming process through four stages includes preparation and centering for backward extrusion, backward extrusion over die pin, upsetting operation, and backward extrusion to form a hexalobular socket over a punch pin. The numerical simulations of cold forming are carried out using the finite element code of DEFORM-3D. The formability of the workpiece is studied, such as the effect on forming force responses, maximum forming forces, effective stress and strain distributions and metal flow pattern. In the four-stage forming process, in the stages of upsetting and backward extrusion over a moving punch to form a hexalobular socket cavity, the effective stresses in the head of the workpiece are significantly high, and the effective strains are also significantly high due to large deformation. The flow line distributions are also very complex in which the flow lines in the regions of upsetting and backward extruding a hexalobular socket cavity at the head of workpiece are severely bent, highly compacted. For the first stage, the maximum axial forming force of 164.3 kN is the greatest of the four stages, which the workpiece is flattened and centered; while the forming energy of 39.9 J is the smallest of the four stages due to the shortest acted axial forging stroke. However, in the second stage of backward extrusion over a punch tool mounted in the die, the maximum forming force of 55.7 kN is the smallest of the four stages; while the forming energy of 263.6 J is the greatest of the four stages due to the longer acted axial forming stroke. The total maximum axial forming forces from the first to the last stages are 413.5 kN and the total forming energies are about 0.56 kJ.

Keywords: cold forming process, hexalobular socket Torx nuts, formability, forming force.

1. INTRODUCTION

Multi-stage cold forming is used in many industries, particularly in the manufacture of fasteners and special parts. The billet is formed sequentially through multiple stations at high speed. Generally, high mechanical properties, good surface appearance and precision are achieved without further processing. In the cold forming process, the prediction of forming forces and stresses is very important for the design of punches and dies and the selection of forming machines. Many cold forming applications use numerical simulation to predict and analyze the forming design. Altan and Knoerr [1] applied two-dimensional finite element method to investigate suck-in extrusion defects, bevel gear forging, stress analysis of forging tools and multi-stage cold forging design. Joun et al. [2] proposed a numerical simulation technique for the forging process with a spring-attached die. They used a penalty rigid-viscoplastic finite element method with an iterative force balance method and explored the significance of metal flow lines on quality control and the influence of spring-attached dies on metal flow lines and forming load reduction. Roque and Button [3] applied ANSYS commercial finite element software to model a forming operation and developed models to simulate ring compression testing and upsetting operations, a stage in the manufacturing process for automotive starter parts. MacCormack and Monaghan [4] proposed a three-stage cold forming process to form the spline shape of the head of aerospace fasteners and numerically analyzed strain, damage, and flow patterns in three stages.

A multi-stage upsetting method to form a thick and wide flange at the pipe end was developed by Hu and Wang [5]. They analyzed the numerical simulation results and discussed the method of determining the step length. Park et al. [6] used the finite element method to establish a systematic process analysis method for the multi-stage forming of the constant velocity joint outer ring and to analyze the formability of the multi-stage forming process. Farhoumand and Ebrahimi [7] applied the finite element code of ABAQUS to analyze the forward-backward-radial extrusion process and investigated the effects of geometric parameters such as die corner radius and gap height as well as process conditions such as friction on the process. The numerical results were compared with experimental data in terms of forming loads and material flow lines in different regions. The hardness distribution of the longitudinal section of the product was used to verify the strain distributions obtained by numerical analysis. Ji et al. [8] used the numerical code of DEFORM_2D to investigate the cold-forming mechanism of a five-stage extrusion process of shaft parts that were used in gearboxes. The results illustrated that the cold extrusion of the five-stage process was feasible and the forming rules were obtained. Paćko et al. [9] presented an application of finite element analysis in the prediction and optimization of bolt forming process. They studied bolt forming process consists of six stages, including shearing, three upsetting stages, backward extrusion, and trimming and proposed and analyzed several tool modifications using numerical simulation. Yang and Lin [10] conducted numerical and experimental investigations on two forming modes of two-step extrusion of AISI 1010 carbon steel. The numerical results of effective strain distributions were consistent with the experimentally measured hardness distributions.

Winiarski and Gontarz [11] proposed a metal-forming process to produce two-step outer flanges on the hollow parts extruded by a movable sleeve. They applied the method to bring the end flange of 6060 aluminum alloy tubular blank and designed this cold-forming process based on numerical simulations and experiments. The experimental results verified the feasibility of cold forging a twostep flange with a diameter approximately twice the outer diameter of the tubular blank. Obiko et al. [12] applied DEFORM 3D to perform three-dimensional finite element analysis to study the plastic deformation behavior of X20CrMoV121 steel during forging process. They studied the effect of forging temperature on the strain, stress and particle flow velocity distribution during forging process. Dubiel et al. [13] introduced the cold forging process of flanged bolts to obtain a consistent, acceptable, and inconsistent grain flow pattern. Then, the FEM simulation results were correlated with the conducted experiments. Lee et al. [14] proposed the use of a multi-stage cold forging process to reduce the manufacturing cost of the solenoid valve while satisfying dimensional accuracy and performance. The forming process is divided into six stages to improve the dimensional accuracy of the armature outer diameter, overall length and slot portion. Szala et al. [15] investigated the hardness behavior and microstructure of 42CrMo4 steel hollow parts with external flanges. Cold forming of metals leads to the work hardening of steels. Metallographic studies verified that flow line arrangement was appropriate, which agreed with that shown by the numerical simulations. The metal forming process did not influence the microstructural uniformity of the flanged hollow parts.

Yang and Liu [16] conducted numerical and experimental studies on a multi-stage cold forming process of AISI 1010 steel relief valve regulating nuts. The numerical simulation of the forming force growth tendency was consistent with the experimental results. The effective strain distributions were consistent with the measured hardness distributions. The highly compact grain flow lines also led to higher hardness. Yang et al. [17] conducted a numerical study on the multi-stage cold forming process for manufacturing eccentric parts of AISI 1022 carbon steel. The formability of the workpiece was numerically investigated. Although the total maximum axial forging load of four-stage forming was less than that of five-stage forming, the maximum lateral forging force in the last stage of fourstage forming was almost 5 times that of the last stage of five-stage forming. Increasing the lateral forging force might cause wear and damage to the punch. Yang et al. [18] presented a numerical analysis of three-stage cold forming process for the manufacture of AISI 316 stainless steel Allen screws and hexalobular socket screws. In the three-stage forming process consisted of twice upsetting and one backward extrusion at the upper face of the workpiece. The effective stresses in the head of the workpiece were significantly high, and the effective strains were also significantly high due to large deformation. Winiarski et al. [19] proposed a method to form flanges in hollow parts. The process consisted of an extrusion with two dies that moved in an opposite direction to that of the punches. This particular kinematics of the tools made it possible to form two flanges simultaneously in a single tool pass. A multi-stage cold forming process for SCM435 alloy steel flange nut manufacture was numerically studied by Yang et al. [20]. The cold forming process through five stages consisted of flattening along with centering, upsetting a hexagonal shape along with backward extrusion, upsetting a flange along with backward extrusion, and piercing. In the five-stage forming process, for the forming stages of upsetting along with backward extrusion and piercing, due to large deformation, the effective stresses in the workpiece were significantly high, and so the effective strains. The flow line distributions were also very complex, particularly in the piercing region. Yang et al. [21] presented a numerical analysis of multi-stage cold forming process for the manufacture of

AISI 316 stainless steel battery bolts. The cold forming process through five stages consisted of preparation and centering, backward extrusion over a die pin, twice upsetting operations, and square trimming. In the five-stage forming process, for the two upsetting and the square trimming forming stages, the effective stresses in the head of the workpiece were significantly high, and the effective strains were also significantly high due to large deformation. The flow line distributions were also very complex, especially in the trimming region of the upset head were severely bent, highly compacted, and eventually fractured due to excessive trimming.

In this study, the numerical simulation of a four-stage cold-forming process for the manufacture of AISI 1022 carbon steel hexalobular socket Torx nuts is presented. The forming process includes preparation and centering for backward extrusion, backward extrusion over a die pin, upsetting operation, and backward extrusion to form a hexalobular socket over a punch pin. The numerical simulation of cold forming is conducted using the finite element code of DEFORM-3D. The forming load responses are calculated and the metal flow pattern, effective stress and effective strain at various deformation zones are analyzed.

2. MATERIALS AND METHODS

The manufacturing process of the hexalobular socket Torx nuts is multi-stage cold forming through four stages. A cold-forging quality AISI 1022 carbon steel wire coil is used in the cold-forming analysis. The chemical composition of the alloy steel wire is shown in Table 1.

Table 1: Chemical composition of AISI 1022 carbon steel wires (wt.%).

C	Mn	P	S	Si	Cu	Ni	Cr	Al
0.22	0.77	0.013	0.007	0.04	0.06	0.01	0.04	0.034

The numerical study of cold forming is conducted using the finite element code of DEFORM-3D. The material is first cut into the desired-length billet through plastic shearing. A billet of ϕ7.85mm × L13.2mm is numerically cut by the shearing die and transfers to forming stations. The threedimensional and cross-section views for initial billet and product parts of five stages are shown in Figure 1.

Both the ends of the cutoff billet are visibly deformed, as shown in Figure 1, due to cutting to length by shearing. The initial billet is no longer an axisymmetric cylindrical body. For the first stage, as shown in Figures 1(a) and 1(b), the process includes flattening the billet end and centering for the backward extrusion in the second stage. In the second stage, a cavity of ϕ5.57 mm is formed at the bottom end with a depth of 10.2 mm by using a punch tool mounted in the die and with a reduction in area of 50.9% for the backward extrusion. Then, the workpiece is moved to the third stage in which the upper end of the workpiece is upset into an approximately cylindrical shape with a height of 4.1 mm. In the final stage, a cavity of hexalobular socket is backward extruded by a moving punch at the head with a depth of 2.2 mm. The deformation energy is

$$E = \int_0^{\Delta L} F dl \quad (1)$$

where F is forming force and ΔL is total acted forging stroke.

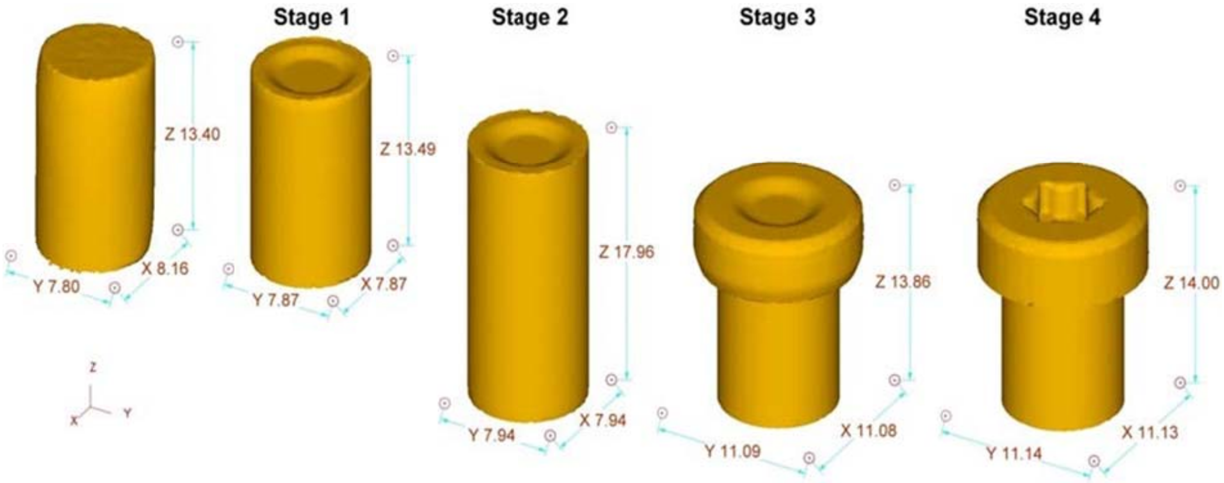

(a) 3D views

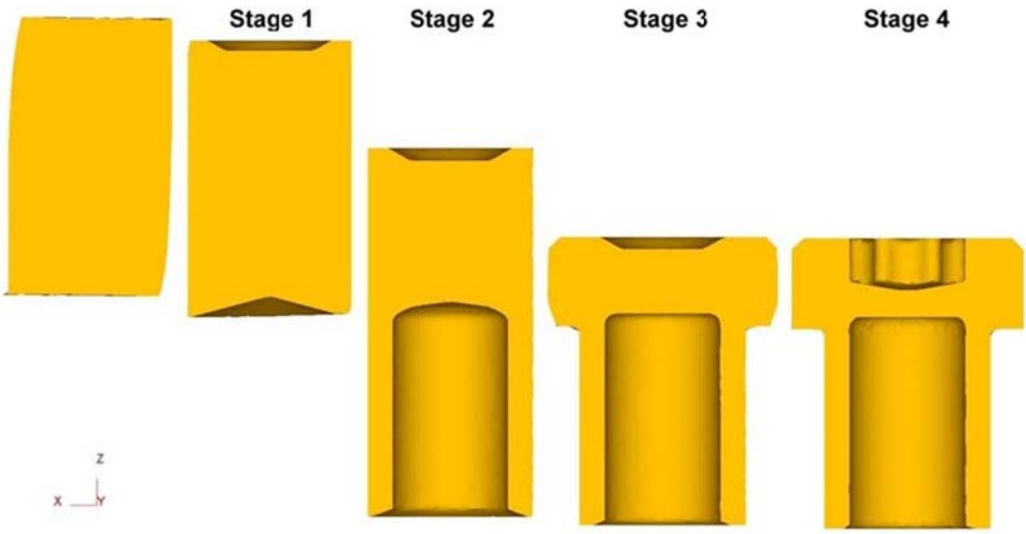

(b) cross-section views

Figure 1: The shapes for initial billet and product parts of each stage.

The numerical simulation of multi-stage cold forming is modeled as a 3D finite element analysis using DEFORM 3D. The workpiece is modeled using tetrahedral elements. The deformations of punches and dies are ignored and treated as rigid objects since their materials are usually much harder than the material of workpiece. The workpiece material is an AISI 1022 carbon steel billet which is considered as a rigid-plastic material with Von Misses yield criterion, isotropic hardening. To obtain more accurate simulation result, a cylindrical compression test, with the specimens of ϕ12.45mm × L15.9mm, is conducted in a 20 tonne universal testing machine under a constant ram speed of 3 mm/min at room temperature, and the following equations are used to obtain the true stress and true strain [22],

$$\sigma = P/A_0, \quad (2)$$

$$\varepsilon = (h - h_0)/h_0, \quad (3)$$

$$\sigma_t = \sigma\,(1 + \varepsilon) = \sigma\,(h/h_0), \tag{4}$$

$$\varepsilon_t = ln(1 + \varepsilon) = ln(h/h_0), \tag{5}$$

where σ is engineering stress, ε is engineering strain, P is compression force, A_0 is initial crosssectional area, h_0 is initial height, h is the instantaneous height, σ_t is true stress and ε_t is true strain. Figure 2 shows the true stress-true strain diagram of AISI 1022 carbon steel, which will be imported into the numerical code of DEFORM to conduct the forming simulation analysis.

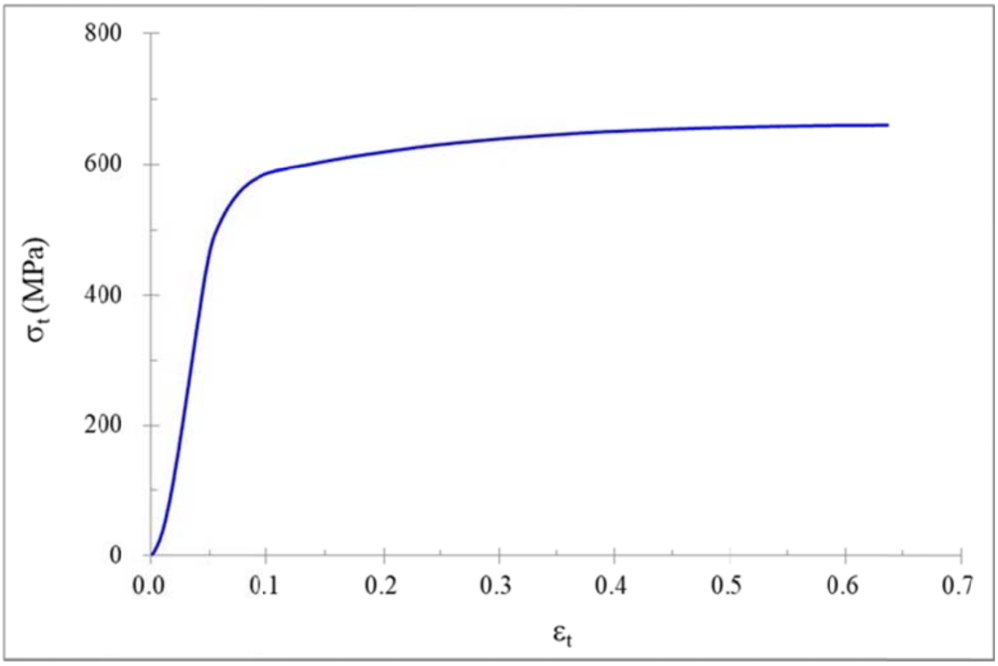

Figure 2: True stress-true train curve of AISI 1022 steel by compression test.

The friction between the workpiece and tools is considered as constant shear friction, and the friction coefficient for cold forming is m = 0.12. The relevant simulation settings are listed in Table 2.

Table 2: Simulation parameters in DEFORM.

Workpiece material	**AISI 1022**
Workpiece/die property	Plastic/rigid
Temperature	20°C
Mesh number	55,000
Mesh element type	Tetrahedron
Friction model/friction coefficient	Constant shear friction/0.12

3. COLD FORMING OF HEXALOBULAR SOCKET TORX NUTS

A numerical study is carried out for the multi-stage cold forming of hexalobular socket Torx nuts through four stages. The effects of forming force responses, maximum forming loads, effective stresses and effective strain distributions, and metal flow patterns are investigated.

3.1 The Forming Load Response and Deformation Energy

The four-stage forming simulation results are shown in Figure 3 for the axial forces. The maximum forming forces are indicated for each stage. The axial forming stroke (ΔL) and deformation energy (E) for each stage are listed in Table 3.

For the force responses of forming force during all stages, it is observed that at first stage the maximum axial forming force is 164.3 kN which is the greatest of the four stages, where there is only a minor deformation to remove the sharp cutting edges and to center for the backward extrusion. Thus, the acted axial forging stroke is only 1.52 mm and the forming energy of 39.9 J is the smallest of the four stages, as shown in Table 3, due to the shortest axial forging stroke. In the second stage, the forming force increased to a maximum of 55.7 kN to backward extrude by a punch tool mounted in the die, with a reduction in area of 50.9% to form the cavity of ϕ5.57 mm and 10.2 mm in depth. The forming energy is 263.6 J, as shown in Table 3, which is the greatest of the four stages due to the longer acted axial forming stroke of 5.37 mm. In the third stage, it upsets a head into an approximately cylindrical shape with a height of 4.1 mm, in a maximum forming force at 122.4 kN which is the second greatest of the four stages, as shown in Figure 3, and the forming energy of 188.6 J, as shown in Table 3, which is the second greatest. At the last stage, a cavity of hexalobular socket is backward extruded by a moving punch at the head to a depth of 2.2 mm and the maximum axial extruding force is 71.2 kN, as shown in Figure 3, while the forming energy of 68.3 J is smaller than those of the second and third stages due to shorter acted axial forming stroke of 1.99 mm, as shown in Table 3.

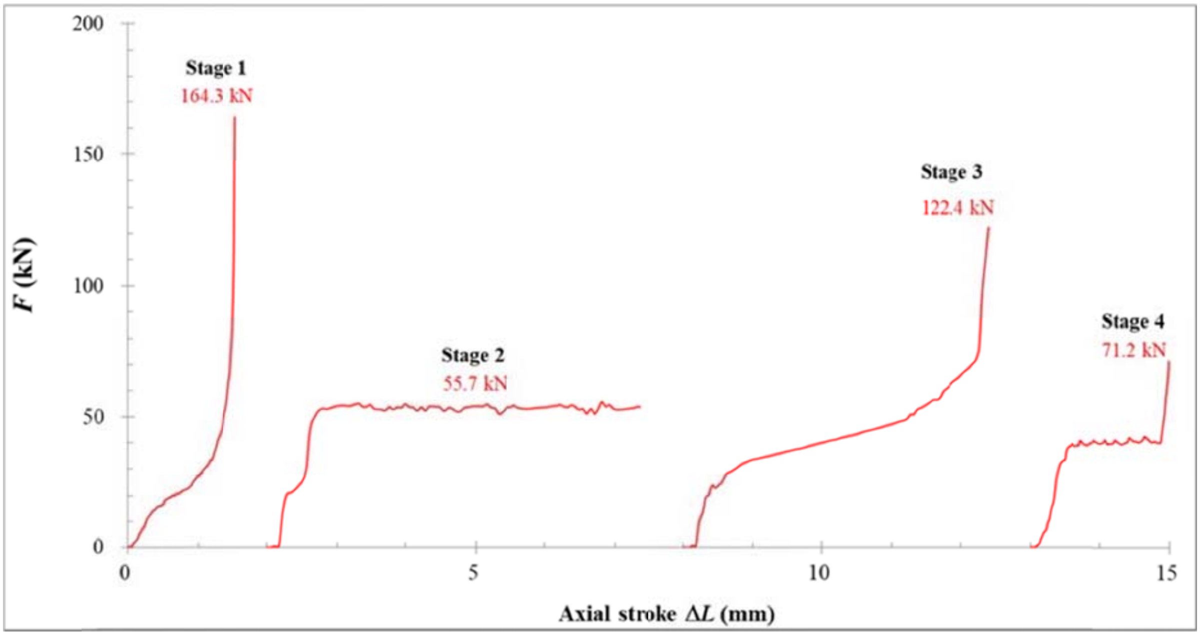

Figure 3: Axial Forging responses for four-stage forming.

For the maximum axial forming force, as shown in Figure 3, the first stage, which the workpiece is flattened and centered (Figure 1), is the largest among the four stages. For the forming energy, as shown in Table 3, the second stage, which a cavity is backward extruded at the bottom end by a punch tool mounted in the die. (Figure 1), is the largest among the four stages due to longer acted axial forming stroke. Overall, the total maximum axial forming forces from the first to the last stages are 413.5 kN; and the total forming energies shown in Table 3 are about 0.56 kJ.

Table 3: The acted axial forging stroke (ΔL) and deformation energy (E) for each stage.

Stage	1	2	3	4	Total
E (J)	39.9	263.6	188.6	68.3	560.3
ΔL (mm)	1.52	5.37	4.40	1.99	

3.2 The Effective Stress Analysis

Figure 4 shows the effective stress distributions at the final position of each stage for the four-stage forming and indicates the maximum effective stresses. For the first stage, stresses are arising at the upper and lower ends of workpiece when they are in contact with the dies, then the stresses increase as the forging load increases, the maximum effective stress is 758 MPa. It is observed that the highest value of effective stress occurs in the upper and lower ends whereas the lowest effective stress occurs in the middle region of workpiece. For the second stage which involves backward extrusion over a die pin, it is analyzed from Figure 4 that the effective stresses are high in the backward-extrusion deformation region. This causes the formation of a cavity at lower face under high pressure in turn causes high effective stress of 756 MPa on workpiece and tool surface. The stress response in the backward extrusion region of workpiece is obviously larger, as shown in Figure 4.

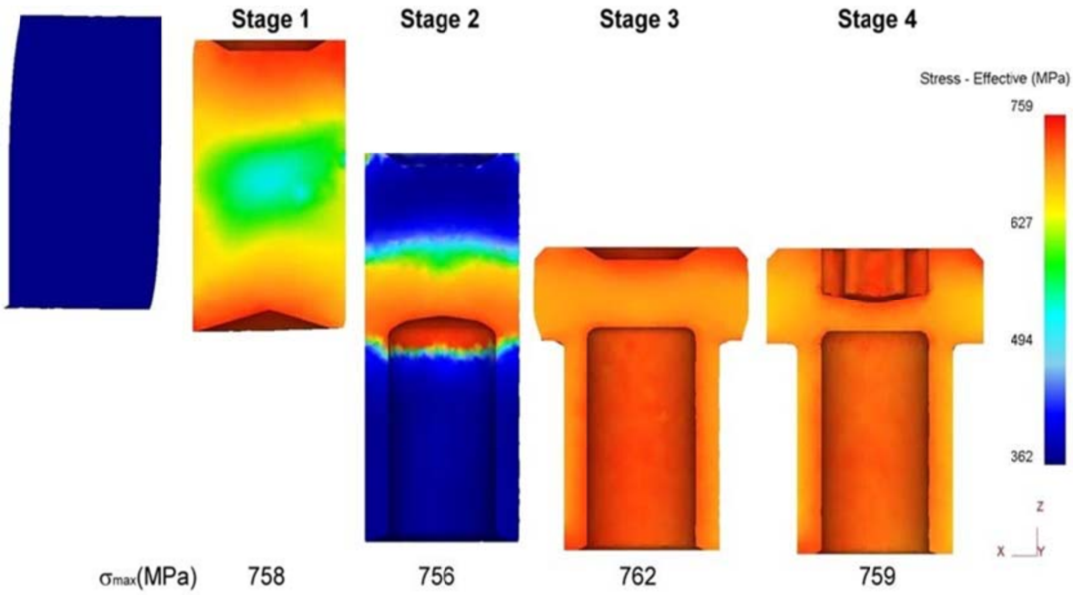

Figure 4: The effective stress distributions at the final position of each stage.

For the third stage which involves the upsetting into an approximately cylindrical shape with a height of 4.1 mm, stresses are arising in the upsetting region and at the lower end of workpiece when they are in contact with the dies, then the stresses increase as the forming load increases. The stress response is significantly larger for almost the head of workpiece, as shown in Figure 4. It is observed that the highest value of effective stress occurs in the upsetting region and at the top end of bottom cavity. The maximum effective stress is 762 MPa. In the fourth stage, the process of backward extrusion over a moving punch is carried to form a cavity of hexalobular socket at the head. This brings about a large deformation in the head of workpiece under high pressure, resulting in high effective stress of 759 MPa, as shown in Figure 4.

3.3 The Effective Strain Analysis

The effective strain distributions at the final position for the four stages are shown in Figure 5. In the first stage, the effective strains in flatting (upper) and centering (lower) regions of workpiece are higher than the middle region where the deformation is small. The effective strain distributions are not completely symmetric due to the visible deformation to the ends of the cutoff billet, as shown in Figure 5. For the second stage of backward extrusion over a die pin at the lower end, the effective strains are high in the upper end and the region of backward extrusion forming with large deformation, as shown in Figure 5. The region with higher effective strains increases along the die pin due to the friction resistance on the contact surfaces between die pin and workpiece.

For the third stage of upsetting into a cylindrical head over a moving punch, the effective strains are high in the upsetting region with large deformation and in the lower region compression over a die pin, while the effective strains of the other region are relatively small, as shown in Figure 5. However, even if the first three stages are axisymmetric forming, their effective strain distributions are obviously not axisymmetric, as shown in Figure 5, since the initial billet is not an axisymmetric cylindrical body. In the fourth stage, the process of backward extrusion over a moving punch is conducted to form a cavity of hexalobular socket at the head and the effective strains are higher in the backward-extrusion region, as shown in Figure 5, while the effective strains of the other region are relatively small.

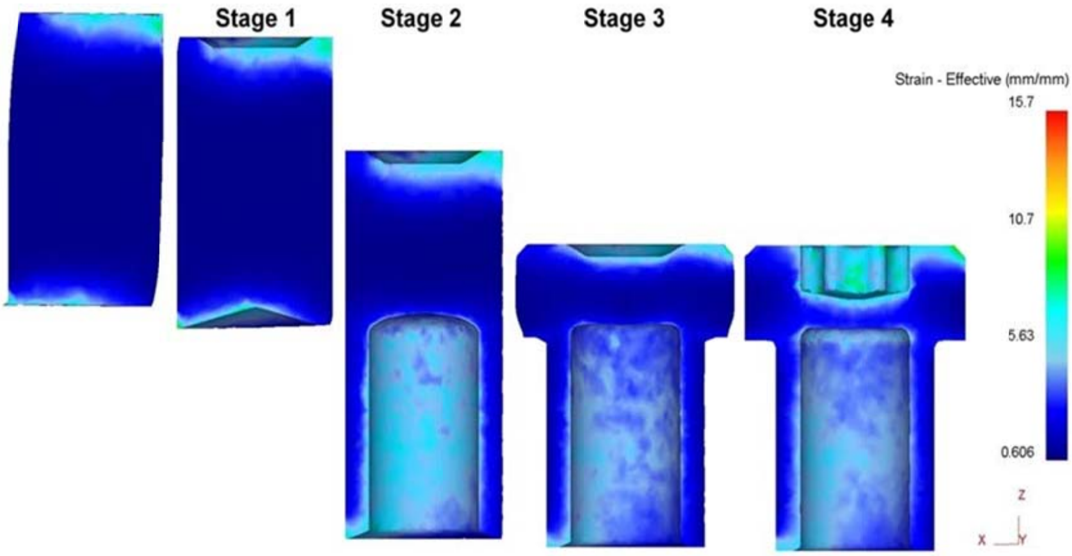

Figure 5: The effective strain distributions at the final position of each stage.

3.4 The Flow Line Analysis

The deformed grains and inclusions in the cold-formed metal are distributed in a bands along the main deformation direction of the metal to form the grain flow lines. The simulation results of flow lines are shown in Figure 6 for the four-stage forming. The flow lines in the initial billet are almost evenly distributed, as shown in Figure 6, except at both ends where the flow lines are vertically bent and highly compacted due to shear deformation. The compactness of the flow lines responses the degree of hardness. Highly compacted flow lines indicate higher hardness [16].

In the first stage, the flow lines in flatting and centering regions of workpiece are highly compacted, as shown in Figure 6; while in the middle region with small deformation, the flow line distributions almost remain uniform. For the second stage of backward extrusion over a die pin at the lower end, the flow lines in the inner wall of the lower cavity are obviously highly compacted due to severe structure deformation, as shown in Figure 6. For the third stage of upsetting into a cylindrical head over a moving punch, the flow lines in the upper and lower regions of upsetting head are obviously curved and highly compacted, as shown in Figure 6. For the fourth stage of backward extruding a cavity of hexalobular socket at the head of the workpiece, the flow lines in the inner wall of the hexalobular socket cavity are more highly compacted and heavily curved in the bottom region of the cavity, as shown in Figure 6. Highly compacted flow lines indicate hardness increased. There is lack of cutting or fracture of the flow lines during the forming process.

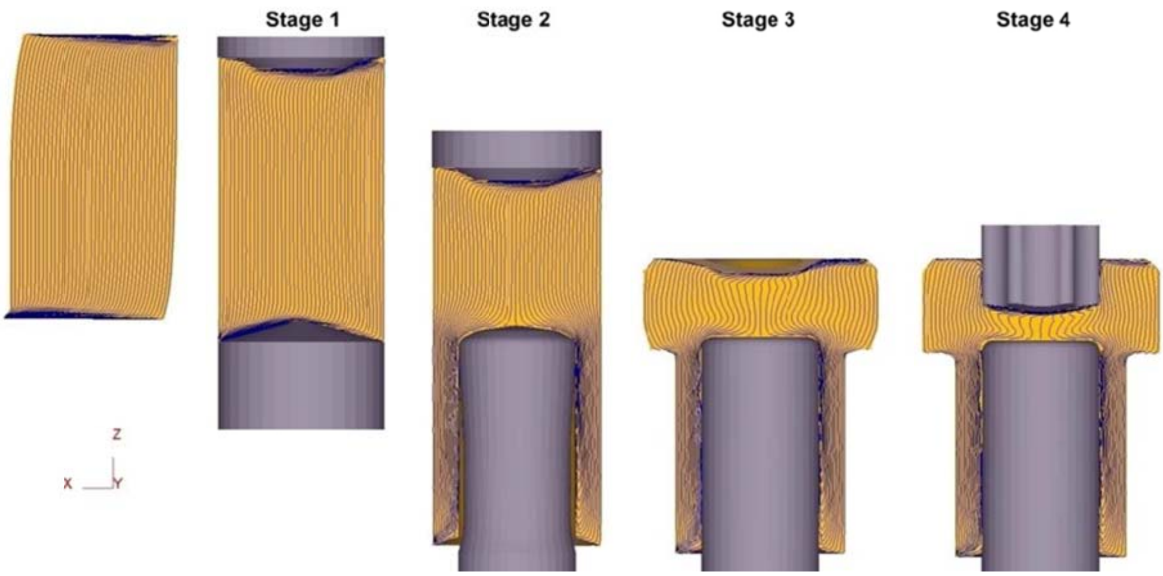

Figure 6: The simulation results of flow lines at the final position of each stage.

4. CONCLUSIONS

A multi-stage cold forming process for the manufacture of hexalobular socket Torx nuts is studied numerically with AISI 1022 carbon steel. The cold forming process through four stages includes preparation and centering for backward extrusion, backward extrusion over a die pin, upsetting operation, and backward extrusion to form a hexalobular socket over a punch pin. The numerical simulations of cold forming are carried out using the FE code of DEFORM-3D. The formability of the workpiece is studied, such as the effect on forming force response, maximum forming force, effective stress and strain distributions, and metal flow pattern.

For the first stage, the maximum axial forming force of 164.3 kN is the greatest of the four stages, which the workpiece is flattened and centered; while the forming energy of 39.9 J is the smallest of the four stages due to the shortest acted axial forging stroke of 1.52 mm. However, in the second stage of backward extrusion by a punch tool mounted in the die, the maximum forming force of 55.7 kN is the smallest of the four stages, while the forming energy of 263.6 J is the greatest of the four stages due to the longer acted axial forming stroke of 5.37 mm. Overall, the total maximum axial forming forces from the first to the last stages are 413.5 kN and the total forming energies are about 0.56 kJ.

For the four-stage forming process, in forming stages of upsetting and backward extrusion over a moving punch to form a hexalobular socket cavity, the effective stresses in the head of the workpiece are significantly high, and the effective strains are also significantly high due to large deformation. In particular, the maximum effective stress in the third stage, the process of upsetting into a cylindrical head, is 762 MPa, which is the largest among the four stages. The flow line distributions are also very complex in which the flow lines in the regions of upsetting and backward extruding a hexalobular socket cavity at the head of workpiece are severely bent, highly compacted. However, even if the four stages are axisymmetric forming, their effective strain and flow line distributions are obviously not axisymmetric since the initial sheared billet is not an axisymmetric cylindrical body.

References

[1]. Altan, T. and Knoerr, M., Application of the 2D Finite Element Method to Simulation of Cold Forging Processes. Journal of Materials Processing Technology, 1992. 35: p. 275–302.

[2]. Joun, M.S.; Lee, S.W.; Chung, J.H., Finite element analysis of a multi-stage axisymmetric forging process. International Journal of Machine Tools and Manufacture, 1998. 38: p. 843-854.

[3]. Roque, C.M.O.L. and Button, S.T., Application of the finite element method in cold forging processes. Journal of the Brazilian Society of Mechanical Sciences, 2000. 22(2): p. 189-202.

[4]. MacCormack, C. and Monaghan, J., 2D and 3D finite element analysis of a three stage forging sequence. Journal of Materials Processing Technology, 2002. 127: p. 48–56.

[5]. Hu, X.L.; Wang, Z.R., Numerical simulation and experimental study on the multi-step upsetting of a thick and wide flange on the end of a pipe. Journal of Materials Processing Technology, 2004. 151(1): p. 321 – 327.

[6]. Park, K.S.; VanTyne, C.J.; Moon, Y.H., Process analysis of multistage forging by using finite element method. Journal of Materials Processing Technology, 2007. 187 – 188: p. 586-590.

[7]. Farhoumand, A. and Ebrahimi, R., Analysis of forward – backward-radial extrusion process. Materials & Design, 2009. 30: p. 2152-2157.

[8]. Ji, D.S.; Jin, J.S.; Ma, W.J.; Xia, J.C.; Xia, H.G.; Dong, Y., Multistage Cold Extrusion Process and Forming Rules of Shaft Parts Used in Gearbox. Advanced Materials Research, 2010. 148-149: p. 683 – 687.

[9]. Paćko, M.; Sleboda, T.; Macioł, S.; Packo, P., Optimization of a Bolt Forming Process by Means of Numerical Simulation. Steel Research International, 2012.

[10]. Yang, C.-C. and Lin, X.-Y., The Forming Analysis of Two-stage Extrusion for 1010 Fastener. Journal of Mechanical Engineering and Automation, 2016. 6: p. 43-45.

[11]. Winiarski, G.; Gontarz, A., Numerical and Experimental Study of Producing Two-Step Flanges by Extrusion with a Movable Sleeve. Archives of Metallurgy and Materials, 2017. 62(2): p. 495–499.

[12]. Obiko, J.O.; Mwema, F.M.; Bodunrin, M.O., Finite Element Simulation of X20CrMoV121 Steel Billet Forging Process Using the Deform 3D Software. SN Applied Sciences, 2019. 1(9).

[13]. Dubiel, T.; Balawender, T.; Osetek, M. The Fibrous Structure of the Bolt and Its Effect on the Joint Reliability. Archives of Metallurgy and Materials, 2021. 66: p. 1075–1085.

[14]. Lee, H.-S.; Park, S.-G.; Hong, M.-P.; Kim, Y.-S., Process design of multi-stage cold forging with small size for ESC solenoid valve parts. Journal of Mechanical Science and Technology, 2022. 36: p. 359-370.

[15]. Szala, M.; Winiarski, G.; Bulzak, T.; Wójcik, Ł. Microstructure and Hardness of Cold Forged 42CrMo4 Steel Hollow Component with the Outer Flange. Adv. Sci. Technol. Res. J. Advances in Science and Technology Research Journal, 2022. 16(4): p. 201–210.

[16]. Yang, C.-C. and Liu, C.-H., The Study of Multi-Stage Cold Forming Process for the Manufacture of Relief Valve Regulating Nuts. Applied Sciences, 2023. 13(10), 6299.

[17]. Yang, C.-C.; Sumampow, Y.; Cruz, S.N.D., The Cold Forming Analysis of Eccentric Parts. European Journal of Applied Sciences, 2023. 11(3): p. 407-421.

[18]. Yang, C.-C.; Nguyen, T.V.; Andres, J.C., The Cold Forming Analysis of Stainless Steel Socket-Head Screws. European Journal of Applied Sciences, 2023. 11(6): p. 225-237.

[19]. Winiarski, G.; Gontarz, A.; Skrzat, A.; Wójcik, M.; Wencel, S., Analysis of a New Process for Forming Two Flanges Simultaneously in a Hollow Part by Extrusion with Two Moving Dies. Metals, 2024. 14(6), 612.

[20]. Yang, C.-C.; Peng, J.-S; Duan, Y.-S.; Sung, C.-L., The Numerical Study of Multi-Stage Cold Forming Process for the Manufacture of SCM435 Alloy Steel Flange Nuts. European Journal of Applied Sciences, 2025. 13(2): p. 400-411.

[21]. Yang, C.-C.; Vien, T.T.T.; Lin, Y.-S., The Cold Forming Analysis of Stainless Battery Bolts. European Journal of Applied Sciences, 2025. 13(2): p. 72-83.

[22]. Hosford, W.F., Mechanical Behavior of Materials, Cambridge University, NY, USA, 2005.